Pulse electron spin resonance investigation of bismuth-doped silicon: Relaxation and electron spin echo envelope modulation

M. Belli
Laboratorio MDM, IMM-CNR, Via C. Olivetti 2, I-20864 Agrate Brianza, Italy and
Department of Material Science, University of Milano-Bicocca, Via R. Cozzi 53, I-20125 Milano, Italy

M. Fanciulli*
Laboratorio MDM, IMM-CNR, Via C. Olivetti 2, I-20864 Agrate Brianza, Italy
Università degli studi di Milano-Bicocca, Piazza dell'Ateneo Nuovo 1, I-20126 Milano, Italy

N. V. Abrosimov
Institute for Crystal Growth, Max-Born Strasse 2, D-12489 Berlin, Germany
(Received 13 February 2011; revised manuscript received 1 April 2011; published 3 June 2011)

Donors in silicon represent good candidates for the realization of several innovative devices exploiting classical as well as quantum information processing functionalities. Although most of the current work in the field is focused on the technological donors (P, As), the more exotic Bi offers interesting properties due to its nuclear spin and electronic structure. We present a detailed pulsed electron paramagnetic resonance study of the spin-spin and spin-lattice relaxation rates along with a full angular analysis of electron spin echo envelope modulation (ESEEM) spectra in bismuth-doped silicon samples having two different donor concentrations. The measurements were performed up to 40 K. ESEEM spectra provide information on the donor wave function via the leading superhyperfine interactions between donor nuclei and nearby ^{29}Si coordination shells. The assignment of the most intense contributions was made on the basis of the angular variation of ESEEM resonances and elementary considerations on the deep donor states.

DOI: 10.1103/PhysRevB.83.235204 PACS number(s): 76.30.Da, 71.55.Cn, 61.72.uf

I. INTRODUCTION

Following Kane's proposal on the exploitation of phosphorus donors in silicon for the implementation of quantum information processing (QIP),[1] a wealth of fundamental as well as technological developments have made the realization of silicon-based qubits more feasible. The observation of long electron spin relaxation times,[2–4] the identification of precise requirements[5,6] which the P-doped silicon system fulfills (at least at liquid He temperatures), and the development of quantum error correction schemes[7] make donors in silicon a promising system for QIP. One of the requirements necessary for the ultimate realization of quantum computing is the identification of systems where spin coherence is demonstrated over a time period equal to the time necessary for a full spin flip but at a working temperature as close as possible to room temperature. Possible natural candidates are single donors deeper than P or double donors.[8] In particular, among group V donors bismuth (Bi) offers some peculiar properties which may be exploited and has recently attracted renewed interest.[9–11] Compared to the other shallow donors (P, As, Sb), Bi has (i) a deeper $1s(A_1)$ ground state, $E = 70.98$ meV,[12] offering opportunities for operation at higher temperatures; (ii) the biggest nuclear spin, $I = 9/2$, providing a 20-dimensional Hilbert space; (iii) a more confined wave function, leading to a reduction of spin diffusion decoherence and to the possibility of gigahertz operation at zero field. In the present paper, we report on an X-band pulsed electron paramagnetic resonance (EPR) investigation of the temperature behavior of electron spin-lattice and spin-spin relaxation times in Bi-doped bulk silicon crystals with different Bi concentrations, along with a full angular study of two-pulse electron spin echo envelope modulation (ESEEM) spectra.

II. EXPERIMENTAL PARAMETERS

Silicon crystals doped with Bi were grown using a Pedestal growth technique.[13] Samples with two different Bi concentrations, [Bi] $= 4.6 \times 10^{14}$ cm^{-3} (sample 1) and [Bi] $= 4.0 \times 10^{15}$ cm^{-3} (sample 2), were investigated. The Bi concentration was determined by secondary ion mass spectrometry (SIMS), which also revealed surface As contamination (surface concentration of the order of 4.0×10^{18} cm^{-3}) decreasing to a level below the SIMS detection limit of 10^{14} cm^{-3} in the first 4 μm. Pulse EPR investigations were performed with an Elexsys E580 EPR spectrometer equipped with an X-band cavity suitable for continuous wave and pulsed experiments. Magnetic field and microwave frequency were monitored using a nuclear magnetic resonance (NMR) probe and a frequency counter respectively. A continuous flow cryostat operated with liquid He allowed measurements in the temperature range 4–300 K. The cryostat optical window was kept closed so that the experiment could be performed in dark conditions. The temperature fluctuations have always been kept below 0.1 K. The relaxation measurements were performed with standard pulsed sequences:[14] echo decay ($\pi/2$ - τ - π - τ - echo) vs interpulse delay τ for spin-spin relaxation time investigations and inversion recovery (π - τ_{IR} - $\pi/2$ - τ - π - τ - echo) for spin-lattice relaxation time measurements. Two-pulse ESEEM spectra were acquired at 12 K at the highest field line with a dwell time of 8 ns and a 16-step phase cycle. The decay trend was fitted and subtracted from the time domain signal to extract the modulated part.

Before applying Fourier transformation, hamming apodization and zero filling were applied, while the pulse length corresponding to a $\pi/2$ turning angle was tuned to 8 ns at the applied microwave power to obtain a high irradiation bandwidth.

III. RESULTS AND DISCUSSION

A. EPR spectrum

As reported by Feher,[15] the Bi spectrum in Si (100% natural abundance of ^{209}Bi, $I = 9/2$) is characterized by an electron gyromagnetic factor $g = 2.0003$ and a hyperfine coupling constant $A_{\rm iso} = 1.4754$ GHz. This large hyperfine interaction distributes the 10 lines which constitute the EPR spectrum in the range $600 \div 5800$ G for X-band operation, as depicted in Fig. 1. The comparison of spectra acquired at different sample orientations confirms that, similar to other group V donor interactions, the Bi hyperfine interaction is completely isotropic. The experiment and the EASYSPIN[16] simulation of the spectrum are in excellent agreement and show that with X-band excitation the intermediate magnetic field regime leads to unevenly spaced resonance lines. The best fit of field-swept electron spin echo (FSESE) spectra at 12 K reveals a Gaussian full width at half maximum (FWHM) of about 4.0 G for both samples for the line at the highest field. The nominal donor concentration cannot account for such a large linewidth, which can thus be attributed to unresolved superhyperfine interaction with nearby ^{29}Si spins, also responsible for the ESEEM signal described in Sec. III D. The fact that the two concentrations yield approximately the same FWHM is a further proof that the linewidth is not determined by dipolar broadening. Actually, the donor electron wave function extends over several Si lattice parameters, and thus several coordination shells (l) contribute to the linewidth ΔH with terms which depend on the isotropic part of the superhyperfine interaction $a_{\rm iso,l}$ according to the expression $\Delta H \propto \sqrt{\sum_l (\frac{a_{\rm iso,l}}{2})^2}$. The superhyperfine parameters for each shell have been calculated for the cases of P, As, and Sb,

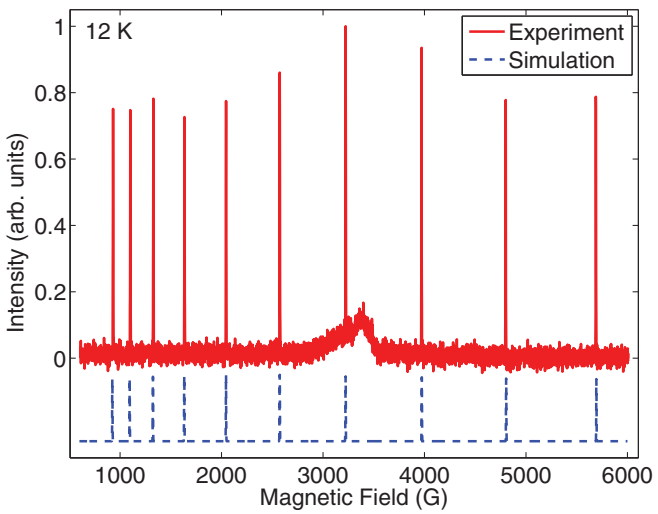

FIG. 1. (Color online) Field-swept electron spin echo (FSESE) EPR spectrum of sample 2 at 9.767921 GHz at 12 K. Both g and hyperfine tensors are isotropic. The blue spectrum represents an EASYSPIN simulation (offset and rescaled for clarity) with parameters taken from the experiment.[16]

and good agreement with electron nuclear double resonance (ENDOR) data was obtained.[15,17,18] However the application of the same theoretical framework for the calculation of the superhyperfine parameters to the case of the deeper Bi donor is questionable.[17] Consequently, the reported difference in the EPR spectrum linewidth should not be ascribed to a simple *rescaling* of the isotropic part of the superhyperfine interaction between donor electrons and nearby ^{29}Si shells calculated for shallow donors. ESEEM data analysis provides information on the wave function and on the superhyperfine couplings (Sec. III D).

The background signal extending in the range $2800 \div 3600$ G (which correspond to g factor in the range $1.95 \div 2.5$) is attributed to a spurious signal from the resonant cavity and to the signals generated by the surface As contamination. We do not discuss further this feature of the recorded spectrum.

B. Electron spin-spin relaxation time

Typical echo decay and inversion recovery measurements of the relaxation times are reported in Fig. 2, while their temperature dependence taken with $H \parallel [001]$ is shown in Fig. 3. A single-exponential contribution is sufficient to efficiently fit the recovery curves, while it is evident from the shape of the decay curves at low temperature that the echo decay cannot be represented by a single exponential. The deviation from a single-exponential decay function is due to the presence of further dephasing channels, as already observed in Si:P.[4] The two main additional mechanisms leading to echo decay in Si-based systems generally come from spectral diffusion[19–21] (SD) and instantaneous diffusion (ID).[4,22–24] The former is due to the spin flip of nonresonant spin species as a consequence of their interaction with the irradiated ones. The resulting slight variation of the local magnetic field experienced by the

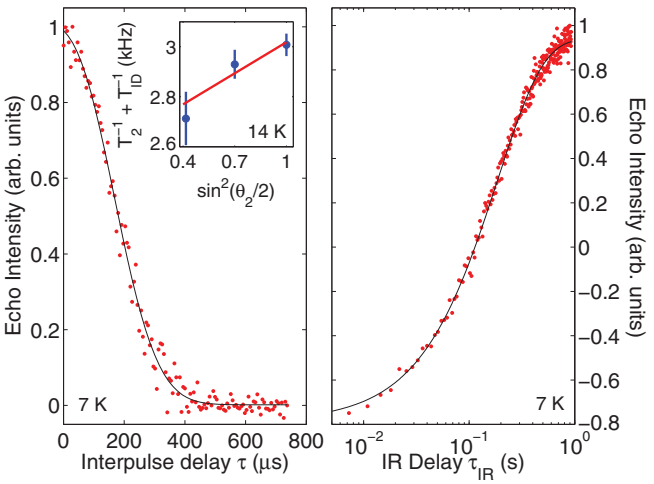

FIG. 2. (Color online) Examples of echo decay (left) and inversion recovery (right) measurements in Si:Bi, along with the corresponding best-fit functions. Inset: echo decay rates taken with $H \parallel [001]$ after subtraction of the spectral diffusion contribution for different values of the second pulse turning angle θ_2 for sample 2 at 14 K. The linear slope is 460 ± 80 Hz at 12 K and 415 ± 40 Hz at 14 K, which yield a weighted average of 423 ± 35 Hz. This value corresponds to a Bi concentration of $(5.1 \pm 0.4) \times 10^{15}$ cm^{-3}. A similar analysis on a sample from the same batch returns $(3.2 \pm 0.3) \times 10^{15}$ cm^{-3}.

probed electrons induces a spread in the resonance frequency, leading to spin dephasing. The theoretical calculation[21] of the effect of spectral diffusion on the echo decay measurements in the case of phosphorus-doped silicon predicted a contribution to the echo decay which follows a stretched exponential behavior with a stretched exponent $n = 3$ (expressing the echo intensity as $\propto \exp[-(2\tau/T_{SD})^n]$). The limit value of the spectral diffusion relaxation rate at low temperature (7 K) is 2.1×10^3 s^{-1} while the corresponding value for P is 3.0×10^3 s^{-1}.[4] The comparison between the two values brings one to conclude that despite the larger EPR linewidth (due unresolved superhyperfine interaction with nearby ^{29}Si nuclei), the increased localization of the Bi electron wave function with respect to shallower donors (P) reduces the overall effect of spectral diffusion, leading to 40% longer T_2, a result in agreement with recently reported data.[10] The effect of the instantaneous diffusion, on the other hand, is intrinsic in spin-spin relaxation measurements based on the pulsed echo technique. The modulation of the dipolar couplings between electron spins caused by the microwave pulses contributes to the echo decay with a simple exponential term which can be distinguished from the intrinsic part (T_2^{-1}) by substituting the echo inversion pulse θ_2 with turning angles different from π. Under the assumption of full line excitation, the following equation [Eq. (1)] holds:[14,22–24]

$$T_{\mathrm{ID}}^{-1} = b_{\mathrm{ID}} \cdot \sin^2\left(\frac{\theta_2}{2}\right) = \frac{\pi}{9\sqrt{3}} \frac{\mu_0 g^2 \mu_B^2}{\hbar} [C] \sin^2\left(\frac{\theta_2}{2}\right). \quad (1)$$

T_{ID}^{-1} represents the instantaneous diffusion contribution to the simple exponential relaxation rate, $[C]$ represents the effective (irradiated) spin concentration, while μ_0 and μ_B represent silicon magnetic permeability (approximated to $4\pi \times 10^{-7}$ H m^{-1}) and Bohr's magneton respectively.

In order to take into account and discriminate between the different contributions to spin-spin relaxation, the echo decay data were fitted with the following model:

$$I = I_0 \cdot \exp[-2\tau \cdot (T_2^{-1} + T_{\mathrm{ID}}^{-1}) - (2\tau/T_{\mathrm{SD}})^n], \quad (2)$$

The stretched component due to spectral diffusion was adopted only below 14 K, since at higher temperatures the T_2 values are limited by T_1 relaxation (Fig. 3). The stretched exponent was found to be 2.6 ± 0.4 in the case of sample 1 and 2.4 ± 0.1 in the case of sample 2 (see inset in Fig. 3). The reported n value corresponds to a weighted mean of the different exponent values extracted at different temperatures, while the uncertainty was evaluated from their standard deviation. The underlying assumption is that the true SD stretched exponent is temperature independent, though actually a temperature trend cannot be excluded beyond doubt on the basis of our data. Both values are, within experimental uncertainties, in accordance with the value reported by George *et al.*[10] It is evident that the leading contribution to spin-spin relaxation at low temperature consists of the spectral diffusion mechanism, which is roughly temperature and concentration independent, at least in the investigated ranges.

In sample 1, no evidence of instantaneous diffusion was observed, and hence we infer that the relatively low donor concentration makes the ID mechanism not efficient ($T_{\mathrm{ID}}^{-1} \sim 0$). On the other hand, in the case of sample 2, a linear

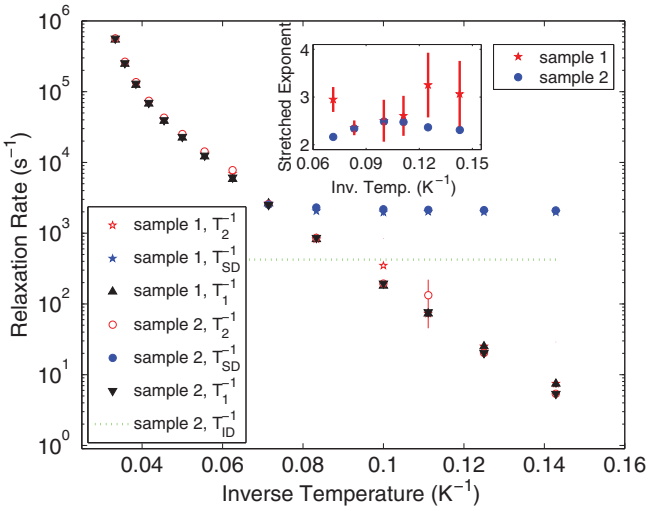

FIG. 3. (Color online) Temperature variation of spin-spin relaxation time taken with $H \parallel [001]$ in sample 1 on the line at the highest field. The spin lattice relaxation rate is reported for comparison. At relatively high temperatures, T_2 is limited by T_1, while below ~14 K they become different. The echo decay is dominated by the temperature-independent spectral diffusion contribution at low temperature, which was fitted as a stretched exponential decay whose exponent is reported in the inset. The relaxation rate values seem roughly independent of the concentration, in contrast with the spectral diffusion exponent.

dependence between the exponential echo decay constant and $\sin^2(\theta_2/2)$ could be measured in the intermediate temperature region where spectral diffusion decay and simple exponential decay become comparable (around $12 \div 14$ K). Since the ID contribution is temperature independent, the extracted ID term (see inset in Fig. 2) was applied and kept constant at all the temperatures investigated in the fitting procedure (Fig. 3). The b_{ID} best fit value is (423 ± 35) Hz, corresponding to a bismuth concentration $[\mathrm{Bi}] = 10 \cdot [C] = (5.1 \pm 0.4) \times 10^{15}$ cm^{-3}. As a further check, a similar analysis was performed on a sample from the same batch as sample 2 and in the same conditions. The concentration extracted from the ID measurement was $(3.2 \pm 0.3) \times 10^{15}$ cm^{-3}. We stress that for both sets of measurements the approximation underlying Eq. (1), that is, full line excitation, is completely valid, since the 24-ns π pulse applied for echo decay measurements was largely enough to achieve the required bandwidth. Consequently, we can state that within experimental uncertainties, the donor concentration extracted from instantaneous diffusion measurements is in agreement with the concentration values measured by SIMS.

C. Electron spin-lattice relaxation time

A study of the electron spin-lattice relaxation rate temperature dependence, measured with $H \parallel [001]$, was performed, in both samples, on the line at the highest field. The T_1 temperature dependence for sample 2 is depicted in Fig. 4. $T_1(T)$ follows the general behavior already reported in the literature,[25–28] and it is well interpreted in the framework of Raman and Orbach relaxation mechanisms. Figure 4 displays also the best fit to Eq. (3):

$$T_1^{-1} = A \cdot T^7 + B \cdot \exp(-\Delta E/k_{\mathrm{B}}T) \quad (3)$$

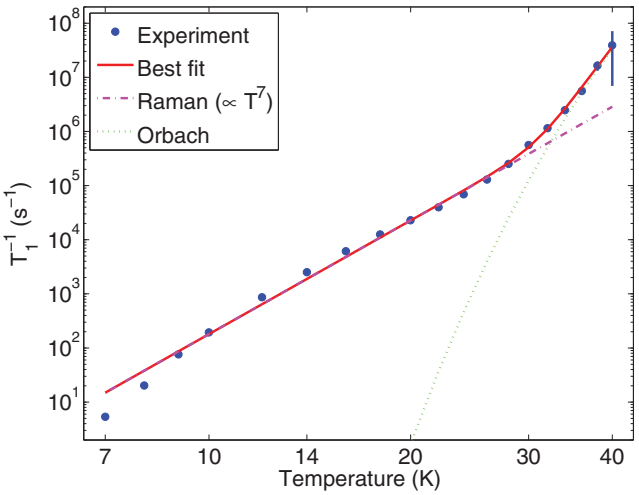

FIG. 4. (Color online) Best fit of the temperature variation of T_1 relaxation rate for the highest field line to Eq. (3) for sample 2. Spin-lattice relaxation is dominated by a power law Raman relaxation, with an Orbach contribution emerging at the higher temperatures.

The dominant contribution comes from the power-law component due to a Raman relaxation mechanism. However, above $26 \div 28$ K also Orbach relaxation begins to emerge.[27] A further term proportional to T did not improve the fitting of the data. Therefore, we conclude that the one-phonon or direct relaxation mechanism is negligible in the investigated temperature range. Despite the relatively low weight of the Orbach component, it is possible to reliably extract the Orbach energy level spacing, at least for the sample with highest Bi concentration, which yields a better signal. The best fit provides the following values: $\Delta E = 57.9 \pm 0.4$ meV, and exponential prefactor $B = (6.6 \pm 0.9) \times 10^{14}$ s^{-1}. Remarkably, the Orbach energy level spacing seems compatible with the splitting between the donor $1s(A_1)$ and $2p_0$ states[12,29,30] instead of the splitting between the $1s(A_1)$ and the $1s(T_2)$ or $1s(E)$ levels as commonly reported for group V donors.[25,28] The observed ΔE value is in agreement with data reported recently.[9] It is worth noting that, in the Bi case, the $1s(A_1)$–$2p_0$ splitting is close to the silicon optical phonons energy. The pre-exponential factor obtained by the best fit is also considerably different from the value reported in the literature.[28] We do not have a clear explanation for these discrepancies, apart from the observation that the extracted Orbach contribution may depend critically on the maximum temperature included in the fitting procedure, which was relatively low in Castner's analysis.

For the sake of completeness, we mention that an Orbach component was included in the fitting procedure also in the case of sample 1, but it did not allow to extract precise values for the fitting parameters. We can state only that the values of B and ΔE fall in the correct order of magnitude ($\Delta E/k_B \sim 800$ K with large uncertainty). On the other hand, the extracted coefficient for the Raman relaxation is estimated as $A = (1.7 \pm 0.1) \times 10^{-5}$ s^{-1} K^{-7} in the case of sample 1 and $A = (1.90 \pm 0.03) \times 10^{-5}$ s^{-1} K^{-7} in the case of sample 2, values which are in fair agreement with those extracted by George *et al.*[10] The power law factor for different donors at different concentrations was reported by Castner.[26] However, these are not readily comparable to our results since the author reported a T^9 spin-lattice relaxation rate dependence, which we do not observe.

The spin-lattice relaxation rates do not show a clear dependence on the concentration. We observed a small variation in the relaxation rates for the two samples only at the lowest temperatures (7 K and 8 K). However, this discrepancy, detected in the temperature range where the spin-lattice relaxation rate has a strong temperature dependence and therefore any temperature uncertainty (of the order of 0.1 K) is quite effective, is only slightly above the experimental error and does not allow us to claim a concentration dependence of the relaxation rates. We point out that a concentration dependence of the spin-lattice relaxation rate is not expected according to the results reported for P by Feher[25] and taking into account the more localized nature of the Bi electronic wave function.

D. Two-pulse ESEEM

ESEEM spectroscopy is a pulsed technique which allows us to probe anisotropic superhyperfine interactions with nearby nuclear spins experienced by the resonant electron spins. In particular, in the case of isotropic donors in natural silicon, the nuclear spins are represented by the ^{29}Si nuclei, which are present with a natural abundance $f(^{29}\mathrm{Si}) = 4.68\%$. The experimental technique consists in the observation of a modulation, originated by the spin dynamics of the nuclei surrounding the paramagnetic center under investigation, in the initial part of the echo decay.[14] The spin Hamiltonian of the interaction between donor electrons and nearby ^{29}Si nuclei can be written as $\mathcal{H}_{\mathrm{shf}} = \sum_l \mathbf{S} \cdot \vec{\mathbf{A}}_l \cdot \mathbf{I}_l$, where the l index runs over all the possible nuclear sites. In its principal axes' frame and under the approximation of axial symmetry, each of the superhyperfine tensors $\mathbf{A}_l$ is diagonal and can be defined by the set of $a_{\mathrm{iso},l}$ and $\tilde{T}_l$ parameters: $\mathbf{A}_l = a_{\mathrm{iso},l} + [-\tilde{T}_l \; -\tilde{T}_l \; 2\tilde{T}_l]$, plus the set of Euler angles defining the tensor orientation in the laboratory frame (α_l,β_l,0). It is useful to define the following quantities:

$$\nu_{\alpha,\beta} = \sqrt{\left(\nu_I \pm \frac{A_\perp}{2}\right)^2 \sin^2\theta_l + \left(\nu_I \pm \frac{A_\parallel}{2}\right)^2 \cos^2\theta_l}, \quad (4)$$

$$\nu_\pm = \nu_\alpha \pm \nu_\beta, \quad (5)$$

where θ_l is the angle between the magnetic field vector and the main axis orientation of the $\mathbf{A}_l$ tensor, ν_I is the nuclear Zeeman frequency, and ν_α and ν_β are the nuclear transition frequencies (the l index has been dropped after each ν symbol to simplify the notation). The theoretical analysis of the modulation of the echo decay for the case of $S = 1/2$ spin states interacting with $I = 1/2$ nuclei (which suits the case of donor electrons and ^{29}Si nuclei) is characterized by frequency components at the four frequencies ν_+, ν_-, ν_α, and ν_β.

Figure 5 shows examples of time-domain two-pulse ESEEM signals detected with the parameters specified in Sec. II, while Fig. 6 displays the angular variation of the frequencies corresponding to the most intense peaks in the ESEEM spectra recorded at 12 K for sample 2, along with the corresponding EASYSPIN simulation.[31] The magnetic field applied during the ESEEM measurements corresponded to the line at the highest field (applied magnetic field ~5690 G). The observed pattern clearly indicates that in the ESEEM spectra at least

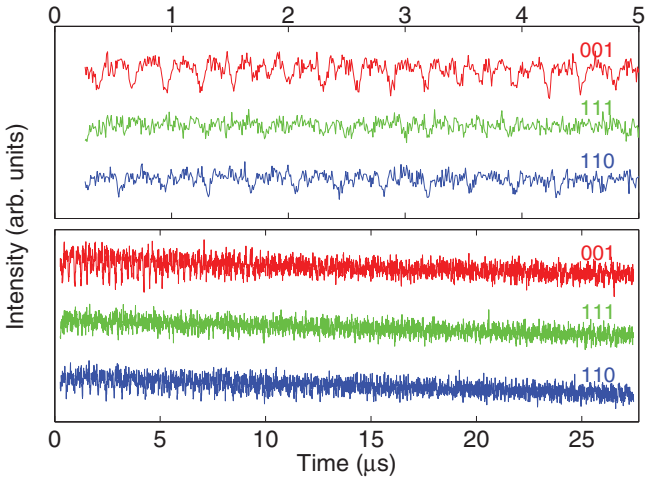

FIG. 5. (Color online) Two-pulse ESEEM signal in time domain for different sample orientations. Data are offset for clarity. The upper part of the figure refers to a zoom on the first 5 μs after the application of the last pulse of the ESEEM pulse sequence.

one shell is present and that it can be unambiguously assigned to the (111) family. The extracted superhyperfine parameters are $a_{\rm iso} = (3.36 \pm 0.03)$ MHz and $\tilde{T} = (2.56 \pm 0.03)$ MHz. The presence of a large anisotropic contribution follows the general trend for (111)-class shells in the cases of other group V donors in Si.[18] In particular, the magnitude of both isotropic and anisotropic contributions allows us to assign the observed shell to the E shell, which is due to the nearest neighbor (111) atoms at a distance of $\sqrt{3} \cdot a_0/4$ from the donor position (a_0 represents the silicon lattice parameter). The small splitting of the doubly degenerate branch [clearly visible along the (001) and nearby directions] can be explained by a slight sample misalignment, which has been taken into account in

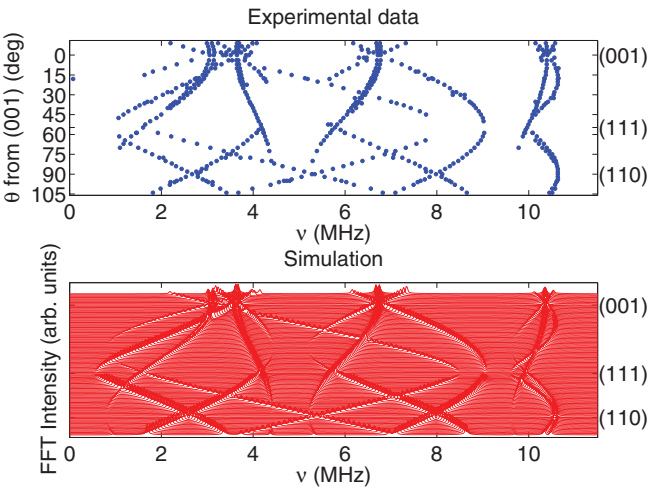

FIG. 6. (Color online) Modulus of the two-pulse ESEEM spectra recorded at different sample orientations for sample 2 at 12 K. The upper panel represents peak positions extracted from experimental data, while the bottom panel is an EASYSPIN[31] simulation with the same parameters taken from the experiment of the ESEEM spectrum due to a single (111)-class coordination shell. A slight sample misalignment is taken into account into the simulation, as explained in the main text.

TABLE I. Shell E superhyperfine parameters for different donors in Si (expressed in kHz). E_I represents the donor ionization energy in meV according to Ref. 12.

Donor	$a_{\rm iso}(E)$	$\tilde{T}(E)$	E_I (meV)	Source
Sb	586 ± 20	522 ± 5	42.74	Ref. 18
P	540 ± 20	700 ± 5	45.59	Ref. 18
As	1284 ± 20	1258 ± 5	53.76	Ref. 18
Bi	3360 ± 30	2560 ± 30	70.98	This work

the simulation. Essentially, the simulated pattern refers to orientations in the plane orthogonal to the [−1 1.0065 0.01] vector, instead of the [−1 1 0] vector, which applies to the case of perfect sample alignment in the laboratory frame. The resulting overall sample misalignment amounts to less than 1°. It is worth noting that the angular ranges where the experimental ESEEM peak intensity falls below the noise threshold in Fig. 6 correspond to the regions where a reduction in the intensity is predicted by the simulation. Experimental data also display other peaks (not shown), most likely generated by different ^{29}Si coordination shells. However, their intensity is very small as compared to the E shell contribution, and hence at present they cannot be unambiguously distinguished from the background noise and assigned. A thorough investigation of these minor peaks will be the subject of further work. In the case of standard shallow donors (P, As, Sb), the most intense shell, as measured by the ENDOR technique, is represented by the A shell,[15] attributed to the (004) sites (expressed in units of $a_0/4$). This fact is not in contradiction with the present measurements on Si:Bi, since the observed ESEEM intensity is directly proportional to the anisotropic part of the superhyperfine tensor and thus the most anisotropic shells are intrinsically more observable than others by the ESEEM technique, independent of the isotropic part of the superhyperfine interaction. The contribution of further shells with larger $a_{\rm iso}$ is actually expected by calculating shell E contribution to the EPR FWHM linewidth, which is roughly $\sqrt{4 f(^{29}\mathrm{Si}) \cdot (\frac{a_{\rm iso}}{2})^2} \cdot 2\sqrt{2 \ln 2} \cdot \frac{h}{g\mu_{\rm B}} \sim 0.6$ G, just 15% of the measured 4.0 G. Noteworthy, the same calculation for shell E in Si:P would yield only 4.5% of the EPR linewidth, confirming the more localized nature of the deep Bi donor electron wave function when compared with the shallower donors (P, As, Sb), as already mentioned in Sec. III A. The available data for shell E parameters for the different group V donor atoms in silicon are reported for comparison in Table I. It can be observed that the $\tilde{T}$ value displays a roughly linear proportionality to the donor ionization energy, and the same applies also to $a_{\rm iso}$, apart from a slight anomaly due to the Sb case. Such a trend is actually expected: A deeper ground state corresponds to a more localized wave function and this leads to an increase of both $|\psi(r_E)|^2$ and the integral in the expression of the electron-nuclear dipole-dipole coupling (proportional to $\tilde{T}$).

IV. CONCLUSIONS

We have investigated electron spin relaxation times and electron spin echo envelope modulation for bismuth in silicon samples having different donor concentrations. The main

mechanism leading to spin-lattice relaxation is a Raman process, though above ∼26 K the phonon density of states begins to allow also for Orbach relaxation, possibly involving the donor $2p_0$ state. Due to the larger ΔE, the Orbach process for Bi sets in at a temperature higher than for P (∼6 K). Regarding spin-spin relaxation, the main contribution involved is spectral diffusion through nearby ^{29}Si spins at temperatures below ∼14 K, where spin-spin relaxation is not limited by spin-lattice relaxation. For the sample with higher Bi concentration, the presence of a concentration-dependent instantaneous diffusion channel was observed. The concentration extracted from the instantaneous diffusion expression in the case of full line excitation is in accordance with the experimental concentration value measured by SIMS, supporting the conclusion that essentially all Bi atoms actually contributed to the ^{209}Bi EPR signal. The Bi concentration also displayed an effect on the determination of the stretched exponent involved in the spectral diffusion contribution to spin-spin relaxation, though no concentration-related effects on T_1 or on the intrinsic T_2 values could be observed. The comparison between the numerical values of the relaxation rates for different donors in silicon allows us to conclude that bismuth extends the possible operating temperature range for future spin-based silicon devices with respect to standard shallow donors like phosphorus. However, deeper donors, as well as isotopically purified Si, will be required to observe a stronger effect and reach relaxation rates, at least above liquid nitrogen temperatures, suitable for QIP. In the case of deeper donors, the electron wave function is expected to be more confined and possibly less influenced by nearby nuclear spins. Dephasing of nuclear origin is still very important in the case of Si:Bi, as evidenced by the dominant spectral diffusion term in spin-spin relaxation and by the presence of a relatively large ESEEM signal. Detailed calculations taking into account substitutional Bi in Si electronic structure are still required to extract the superhyperfine parameters for the various coordination shells, though the most intense peaks in the ESEEM signal at different orientations have been associated to the *E* shell, corresponding to the nearest neighbor (111) sites.

ACKNOWLEDGMENTS

The authors acknowledge H. Riemann for providing the samples and G. Allodi for the FMINUIT minimization package. This work was partly supported by the CARIPLO Foundation National Project ELIOS.

*marco.fanciulli@unimib.it

[1] B. E. Kane, Nature (London) **393**, 133 (1998).
[2] M. Fanciulli, P. Höfer, and A. Ponti, Physica B **342**, 895 (2003).
[3] A. M. Tyryshkin, S. A. Lyon, A. V. Astashkin, and A. M. Raitsimring, Phys. Rev. B **68**, 193207 (2003).
[4] A. Ferretti, M. Fanciulli, A. Ponti, and A. Schweiger, Phys. Rev. B **72**, 235201 (2005).
[5] D. Loss and D. P. DiVincenzo, Phys. Rev. A **57**, 120 (1998).
[6] D. P. DiVincenzo, Fortschr. Phys. **48**, 771 (2000).
[7] J. Preskill, Proc. R. Soc. London A **454**, 385 (1998).
[8] B. E. Kane, N. S. McAlpine, A. S. Dzurak, R. G. Clark, G. J. Milburn, H. B. Sun, and H. Wiseman, Phys. Rev. B **61**, 2961 (2000).
[9] G. W. Morley, M. Warner, A. M. Stoneham, P. T. Greenland, J. van Tol, C. W. M. Kay, and G. Aeppli, Nat. Mater. **9**, 725 (2010).
[10] R. E. George, W. Witzel, H. Riemann, N. V. Abrosimov, N. Nötzel, M. L. W. Thewalt, and J. J. L. Morton, Phys. Rev. Lett. **105**, 067601 (2010).
[11] M. H. Mohammady, G. W. Morley, and T. S. Monteiro, Phys. Rev. Lett. **105**, 067602 (2010).
[12] A. K. Ramdas and S. Rodriguez, Rep. Prog. Phys. **44**, 1297 (1981).
[13] H. Riemann, N. Abrosimov, and N. Nötzel, ECS Trans. **3**, 53 (2006).
[14] A. Schweiger and G. Jeschke, *Principles of Pulse Electron Paramagnetic Resonance* (Oxford University Press, Oxford, 2001).
[15] G. Feher, Phys. Rev. **114**, 1219 (1959).
[16] S. Stoll and A. Schweiger, J. Magn. Reson. **178**, 42 (2006).
[17] J. L. Ivey and R. L. Mieher, Phys. Rev. B **11**, 849 (1975).
[18] E. B. Hale and R. L. Mieher, Phys. Rev. **184**, 739 (1969).
[19] J. R. Klauder and P. W. Anderson, Phys. Rev. **125**, 912 (1962).
[20] M. Chiba and A. Hirai, J. Phys. Soc. Jpn. **33**, 730 (1972).
[21] R. de Sousa and S. Das. Sarma, Phys. Rev. B **68**, 115322 (2003).
[22] A. M. Raitsimring, K. M. Salikhov, B. A. Umanskii, and Yu. D. Tsvetkov, Sov. Phys. Solid State **16**, 492 (1974) [Fiz. Tverd. Tela **16**, 756 (1974)].
[23] A. M. Raitsimring, K. M. Salikhov, S. A. Dikanov, and Yu. D. Tsvetkov, Sov. Phys. Solid State **17**, 2095 (1976) [Fiz. Tverd. Tela **17**, 3174 (1975)].
[24] S. Agnello, R. Boscaino, M. Cannas, and F. M. Gelardi, Phys. Rev. B **64**, 174423 (2001).
[25] G. Feher and E. A. Gere, Phys. Rev. **114**, 1245 (1959).
[26] J. T. G. Castner, Phys. Rev. **130**, 58 (1963).
[27] R. Orbach, Proc. R. Soc. London A **264**, 458 (1961).
[28] T. G. Castner, Phys. Rev. **155**, 816 (1967).
[29] N. R. Butler, P. Fisher, and A. K. Ramdas, Phys. Rev. B **12**, 3200 (1975).
[30] S. G. Pavlov, H.-W. Hübers, M. H. Rümmeli, R. Kh. Zhukavin, E. E. Orlova, V. N. Shastin, and H. Riemann, Appl. Phys. Lett. **80**, 4717 (2002).
[31] S. Stoll and R. D. Britt, Phys. Chem. Chem. Phys. **11**, 6614 (2009).